Mixed-Mode Oscillations in a Modified Chua's Circuit

Wieslaw Marszalek · Zdzislaw Trzaska

Abstract We consider a singularly perturbed system of differential equations of the form $\epsilon u' = g(u, v, \lambda)$, $v' = f(u, v, \lambda)$, where $(u, v) \in R^3$, $0 < \epsilon \ll 1$, and λ is a set of parameters. Such a system describes a modified Chua's circuit with mixed-mode oscillations (MMOs). MMOs consist of a series of small-amplitude oscillations (canard solutions) and large-amplitude relaxations. In the paper we provide a series of both numerical and analytical analyses of the singularly perturbed system for the modified Chua's circuit with nonlinear f and g. In particular, we analyze the occurrence of the *Farey sequence L^s*, where L and s are the numbers of large and small oscillations, respectively.

Keywords Mixed-mode oscillations · Modified Chua's circuit · Singularly perturbed systems

1 Introduction

Recently there has been great interest in the analysis of mixed-mode oscillations (MMOs) consisting of a series of small-amplitude oscillations (also called the sub-threshold oscillations, or STOs) and large-amplitude oscillations, or relaxations, occurring in various patterns. A wide spectrum of dynamical systems with MMOs

W. Marszalek (✉)
College of Engineering & Information Sciences, DeVry University, 630 US Highway 1,
North Brunswick, NJ 08902, USA
e-mail: wmarszalek@devry.edu

Z. Trzaska
Department of Management and Production Engineering, Warsaw University of Ecology and
Management, Wawelska 14, 02-061 Warsaw, Poland
e-mail: zdzislaw.trzaska@netlandia.pl

occurs in biology and chemistry. Such problems include, among others, the burst-
ing dynamics in Taylor–Couette flow, the compartmental Wilson–Callaway model of
the dopaminergic neuron, stellate cell dynamics, the famous Hodgkin–Huxley model
of neuron dynamics, the coupled calcium oscillator model, the complex plasma in-
stability model, and the surface oxidation reaction and autocatalytic chemical re-
action (see [1, 5] for such examples). Electronic circuits exhibiting various types
of MMOs (or close to MMOs) include the coupled *RLC* plus tunnel diode oscilla-
tors [5], autonomous Van der Pol-Duffing equation [6] and transformed Chua's circuit
[3, 10, 16, 17].

All the above physical phenomena are described by singularly perturbed systems
of nonlinear ordinary differential equations (ODEs) with three (or more) variables
changing at different time scales (usually two or three). A cubic nonlinearity is typical
in systems with MMOs. In recent years, the most accepted and popular approach to
explain the MMO phenomenon in R^3 is that the MMOs result from a combination of
canard solutions around a fold singularity and relaxation spikes coupled together by
a special *global return mechanism* [9].

In this paper we shall study a nonlinear circuit which can be called a *modified
Chua's circuit* since its topology resembles that of the original Chua's circuit [4].
The circuit analyzed in this paper has two dual versions, each with a nonlinearity of
a cubic type and a voltage- (current-) controlled voltage (current) source plus a small
biasing constant source.

The paper is organized as follows. In Sect. 2 we present the modified Chua's circuit
and its mathematical description with variables in three time scales. In Sect. 3 we
briefly present fundamental issues of the singularly perturbed systems of ODEs in
relation to the MMOs phenomenon. Then, in Sect. 4, the modified Chua's circuit of
Sect. 2 is analyzed both analytically and numerically. Brief conclusions follow in
Sect. 5.

2 A Modified Chua's Circuit

Consider the circuit shown in Fig. 1(A) (its dual equivalence shown in Fig. 1(B))
with the nonlinear voltage-current characteristics $V_n = \alpha_V x_1^2 + \beta_V x_1^3$ (equivalently
$I_n = \alpha_I x_1^2 + \beta_I x_1^3$ for the dual circuit).

Let the voltage-controlled voltage source (current-controlled current source for the
dual circuit) be described by $V = (1 + b)x_2$ (equivalently $I = (1 + b)x_2$ for the dual
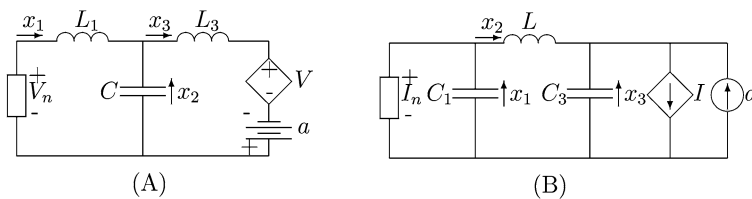
Fig. 1 (**A**) The LCL circuit with $L_1 = \epsilon \ll 1$, $V = (1+b)x_2$, $V_n = \beta x_1^3 + \alpha x_1^2$. (**B**) The CLC circuit with
$C_1 = \epsilon \ll 1$, $I = (1+b)x_2$, $I_n = \beta x_1^3 + \alpha x_1^2$. For both circuits: $a = \text{const.} > 0$, $b = \text{const.} > 0$, $\beta < 0$,
and $\alpha > 0$

circuit) with $b > 0$. The constant biasing voltage (or current) source with $a > 0$ plays a significant role in the creation of MMOs. The following ODEs describe each of the circuits shown in Fig. 1:

$$\gamma_1 x_1' = -x_2 + \alpha x_1^2 + \beta x_1^3,$$
$$\gamma_2 x_2' = x_1 - x_3, \tag{1}$$
$$\gamma_3 x_3' = a - b x_2,$$

where $\gamma_1 \equiv L_1$, $\gamma_2 \equiv C$, $\gamma_3 \equiv L_2$ (and $\gamma_1 \equiv C_1$, $\gamma_2 \equiv L$, $\gamma_3 \equiv C_2$ for the dual circuit). The $\alpha = \alpha_V$ and $\beta = \beta_V$ for the first circuit and $\alpha = \alpha_I$, $\beta = \beta_I$ for the dual one.

Consider the LCL circuit shown above with $0 < L_1 \equiv \epsilon \ll 1$, $C, L_2 \sim \mathcal{O}(1)$. Then (1) can be written in the form

$$\epsilon x_1' = -x_2 + \alpha x_1^2 + \beta x_1^3 \equiv g(x_1, x_2, x_3),$$
$$x_2' = x_1 - x_3 \equiv f_1(x_1, x_2, x_3), \tag{2}$$
$$x_3' = a - b x_2 \equiv f_2(x_1, x_2, x_3).$$

System (2) is a prototypical example for MMOs studied in [9]. Its behavior depends on all five constants (parameters) involved. One can distinguish three different modes (regimes) of operation of (2): only small-amplitude oscillations (SAOs) around the origin, large-amplitude oscillations (LAOs), and a mixture of both SAOs and LAOs which leads to the MMO phenomenon. The three modes are illustrated in Fig. 2, which shows the solutions of (2) with $\epsilon = 0.01$, $\alpha = 1.5$, $\beta = -1$, $b = 0.005$, and three values of a. In the SAOs only case, the SAOs around the origin $(0, 0, 0)$ are due to the Hopf bifurcation for $a = 0$. In the LAOs only case, a trajectory passing close to the origin bypasses the region of SAOs. The MMOs case is in some sense a combination of the previous two cases. The mechanism in which SAOs and LAOs occur is quite complex and has been the topic of recent papers [7–9]. In the MMOs case, a series of SAOs around the origin (considered as canard solutions) undergoes a rapid *canard explosion* yielding an LAO, which, through a special *return mechanism*, brings back the system into the vicinity of the origin. The *canard explosion*, described in detail in [9], is triggered when a trajectory in 2D or 3D cases leaves a fold point of the cubic nonlinearity in (2), ending a series of SAOs and entering the relaxation mode with SAOs. This explosion occurs, for example, in Fig. 2, bottom part, when two or four SAOs transform into an LAO (see x_1 in blue). Depending on the parameters, the system may continue with one (or more) LAOs, or may go through a new series of SAOs, after which the trajectory again leaves the vicinity of the origin and the phenomenon repeats. See Figs. 3 and 4 for illustration.

The *return mechanism* of (2) causes the trajectory leaving the fold of $g(x_1, x_2, x_3) = 0$ (point A in Fig. 5 in the vicinity of the origin) to return to the fold at point E. This mechanism can be analyzed in more detail, after making a number of simplifications and using the reduced system of (2), by the method presented in [9]. In particular, we assume that the mechanism $ABCDE$ in Fig. 5 is approximated by two single arrowed paths only, BC and DE, ignoring the double arrowed ones. One parameter that characterizes such a mechanism is the *amount of return* of variable x_3 in (2) equal to
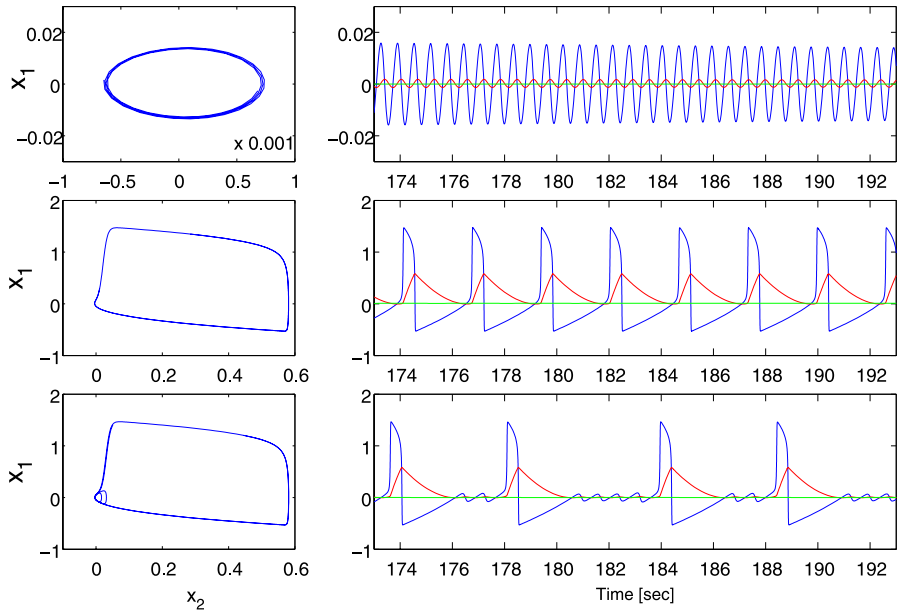
Fig. 2 (Color online) *Left column*: x_1 versus x_2; *right column*: time responses ($172 \leq t \leq 194$); both columns: SAOs only (*top*: $a = 0$), LAOs only (*middle*: $a = 0.00105$), and MMOs (*bottom*: $a = 0.00055$) with x_1 (*blue*), x_2 (*red*), x_3 (*green*)


Fig. 3 In the vicinity of $(0, 0, 0)$: trajectory for $a = 0.00035$ with several SAOs (entering from the left and leaving on the right)
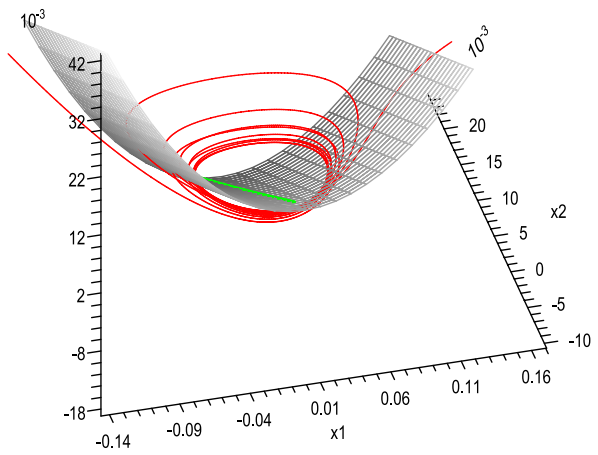
$b\alpha^5/(18\beta^3) - a\alpha^2/\beta$. Closely related to the issue of the *return mechanism* is the critical value of parameter a, that is, $a_c = b\alpha^3/(18\beta^2)$, such that for $a > a_c$ the system exhibits only the LAOs and no MMOs exist. The values a_c and the *amount of return* were obtained by integrating the reduced system of (2) along the single arrowed paths in Fig. 5. The details of the calculations can be found in [9].
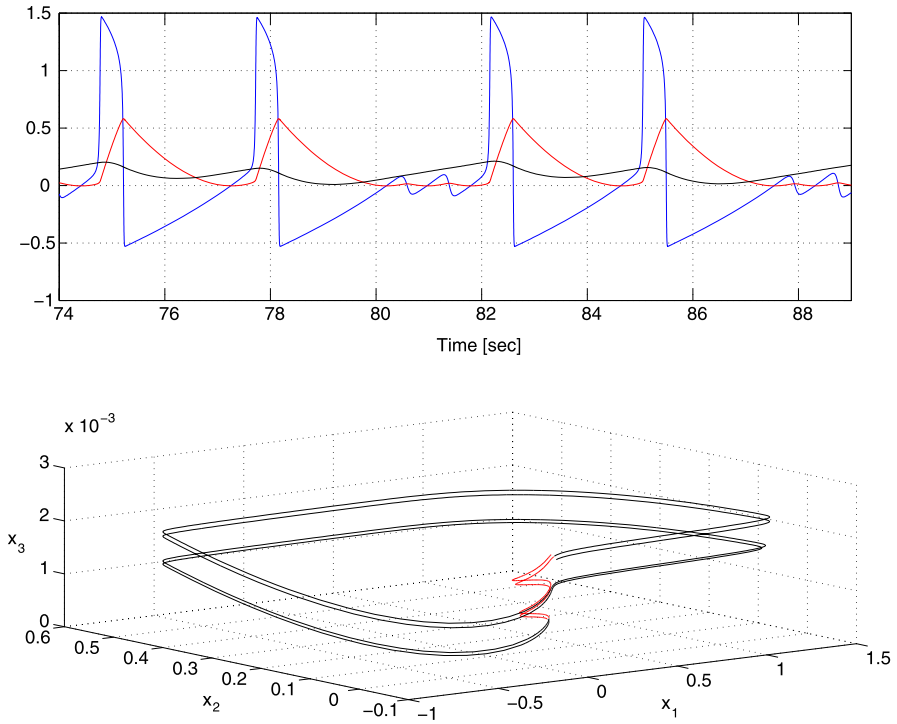
Fig. 4 (Color online) $a = 0.00075$. *Top*: MMOs $2^2 2^2$ with x_1 (*blue*), x_2 (*red*), $100x_3$ (*green*). *Bottom*: 3D trajectory $2^2 2^2$
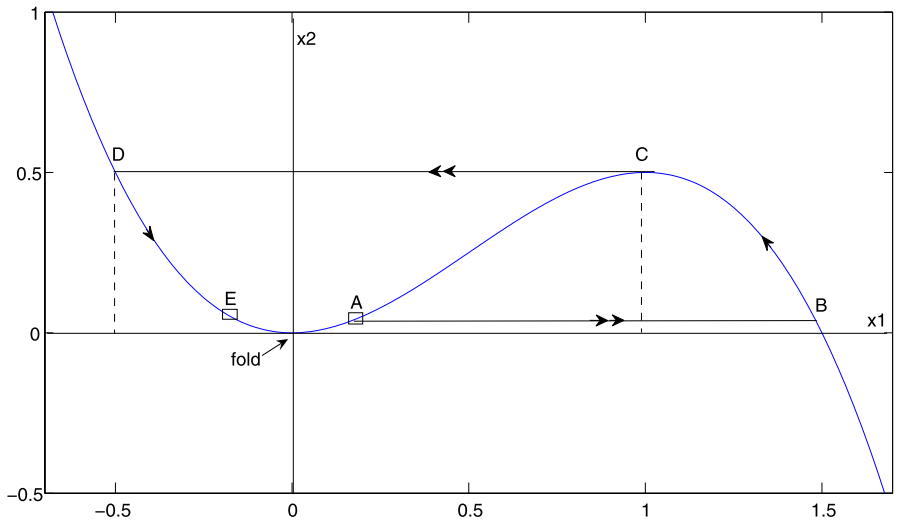
Fig. 5 The schematic diagram of the *Preturn mechanism*
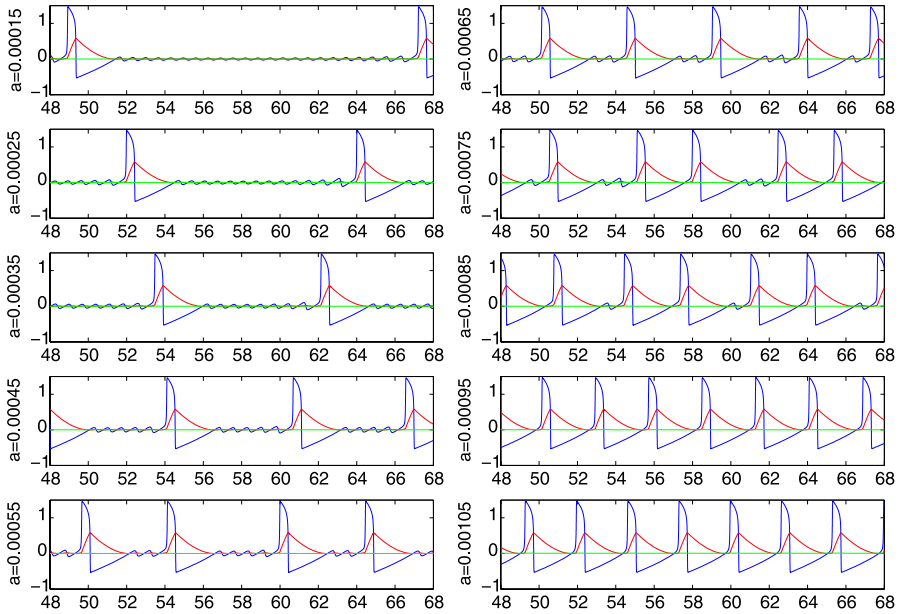
Fig. 6 (Color online) Solutions x_1 (*blue*), x_2 (*red*), and x_3 (*green*) of (2) versus t (seconds) for various values of a

For fixed α and β in (2) the values of a, b, and ϵ are responsible for various types of MMOs. The MMOs are characterized by the *Farey sequence* $L_{k-1}^{s_k-1} L_k^{s_k} L_{k+1}^{s_k+1}$, where L_i and s_i are the numbers of LAOs and SAOs, respectively. Figure 6 illustrates many typical cases that one may obtain from (2). The graphs were obtained by varying parameter a for the fixed values of $b = 0.005$, $\epsilon = 0.01$, $\alpha = 1.5$, and $\beta = -1$. Note that due to the fact that $a \sim \mathcal{O}(\epsilon^2)$, $b \sim \mathcal{O}(\epsilon^2)$, $x_3(t)$ is the *slowest* of all three variables and $x_1(t)$ is the *fastest* one. With the above chosen parameters, system (2) may be called a three-time-scale system.

3 MMOs in Singularly Perturbed System (2)

The MMO phenomenon reported in several biological and chemical systems in recent years seems not to be so common in electrical circuits. The detailed analysis of MMOs in a three-time-scale system presented in [9] is based on the canard phenomenon [2, 7, 8, 15, 18]. Other tools used to explain MMOs are the subcritical Hopf bifurcations, loss of stability of a Shilnikov homoclinic orbit, and a slow passage through a delayed Hopf bifurcation [9].

Let's begin with a brief description of the *desingularized* system in R^3. The *desingularization* process in R^3 is as follows. Let $\epsilon = 0$ and assume that the system

$$
\begin{aligned}
0 &= g(x_1, x_2, x_3), \\
x_2' &= f_1(x_1, x_2, x_3), \\
x_3' &= f_2(x_1, x_2, x_3),
\end{aligned}
\tag{3}
$$

satisfies the following conditions at a point $(x_1^*, x_2^*, x_3^*) \in R^3$ [11, 13]:

$$g(x_1^*, x_2^*, x_3^*) = 0, \qquad g_{x_1}(x_1^*, x_2^*, x_3^*) = 0,$$
$$g_{x_2}(x_1^*, x_2^*, x_3^*) \neq 0, \qquad q_{x_1 x_1}(x_1^*, x_2^*, x_3^*) \neq 0,$$
$$\{g_{x_2} f_1 + g_{x_3} f_2\}_{|(x_1^*, x_2^*, x_3^*)} = 0,$$

where g_{x_i} is the partial derivative of g with respect to x_i.

Then, the critical (constraint) manifold given by the first equation in (3) is given locally as $x_2 = \psi(x_1, x_3)$ and from (3) we have

$$\begin{pmatrix} 1 & 0 \\ 0 & -g_{x_1} \end{pmatrix} \begin{pmatrix} x_3' \\ x_1' \end{pmatrix} = \begin{pmatrix} f_2 \\ g_{x_2} f_1 + g_{x_3} f_2 \end{pmatrix}. \tag{4}$$

The above system is called the *reduced* system. If we multiply the right-hand side of (4) by $-g_{x_1}$ (time rescaling process) and then drop $-g_{x_1}$ from the second equation in (4), then we obtain the corresponding *desingularized* system [12]

$$\begin{pmatrix} x_3' \\ x_1' \end{pmatrix} = \begin{pmatrix} -g_{x_1} f_2 \\ g_{x_2} f_1 + g_{x_3} f_2 \end{pmatrix}. \tag{5}$$

The motivation for forming the *desingularized* equations is the following. Because of the assumptions made, system (5) has an equilibrium at (x_3^*, x_1^*) and the phase portrait of (4) is obtained from that of (5) by reversing the flow of (5) on that side of the fold (also called the impasse) curve where $g_{x_1} > 0$. The usual equilibria of (5), such as the saddles, nodes, and centers, are now called the pseudo-saddles, pseudo-nodes, and pseudo-centers of (4), respectively. Thus, the analysis of the *reduced* equations (4) is, in some sense, equivalent to that of two ODEs in (5) [14].

The complete analysis of the occurrence of MMOs, particularly with regard to the *Farey sequence L^s* for (2), is not available at the present time. However, several known facts and estimates of MMOs will be helpful in our analysis of (2).

(a) First, the MMOs occur in (2) if the origin $(0, 0, 0)$ is a folded node of the *desingularized* system (5). This happens if

$$4b\alpha^3/(27\beta^2) - 1/(8\alpha) < a < b\alpha^3/(18\beta^2). \tag{6}$$

The lower bound for a follows from the fact that (5) has a node at $(0, 0, 0)$ (see Fig. 7), and the upper bound results from the analysis of the *return mechanism* described in [9]. For $a > b\alpha^3/(18\beta^2)$ the system (2) is in a pure relaxation mode with LAOs only.

(b) Second, the period of small oscillations in the vicinity of the fold line $(0, 0, x_3)$ can be estimated by the purely imaginary eigenvalues of a linearized system (2) from which we obtain $\omega = \sqrt{\epsilon^{-1} - b}$; see Sect. 4 for details. Thus, the period of a small oscillation is estimated to be $T = 2\pi/\sqrt{\epsilon^{-1} - b}$.

(c) Third, the number of SAOs and the type of sequence L^s for fixed α and β depend on the initial conditions and parameters a and b. The numerical results of the occurrence of MMOs and the average s values for (2) are presented in the next section.

Folded focus	Folded node	C	Folded saddle

No oscillations A	MMOs	B	Relaxation only
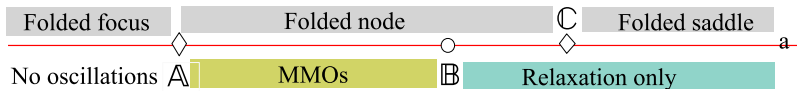
Fig. 7 Intervals of a for various types of responses of (2) with $\mathbb{A} = 4b\alpha^3/(27\beta^2) - 1/(8\alpha)$, $\mathbb{B} = b\alpha^3/(18\beta^2)$, and $\mathbb{C} = 4b\alpha^3/(27\beta^2)$

4 Analysis of MMOs in the Modified Chua's Circuit

Linearizing (2) yields the Jacobian matrix

$$\begin{pmatrix} F'(x_1)\epsilon^{-1} & -\epsilon^{-1} & 0 \\ 1 & 0 & -1 \\ 0 & -b & 0 \end{pmatrix}, \tag{7}$$

where $F(x_1) = \alpha x_1^2 + \beta x_1^3$, and the eigenvalues satisfying the characteristic equation

$$\lambda^3 + P\lambda^2 + Q\lambda + R = 0, \tag{8}$$

where $P = -F'(x_1)\epsilon^{-1}$, $Q = \epsilon^{-1} - b$, and $R = F'(x_1)b\epsilon^{-1}$.

The Hopf locus is obtained for $R - PQ = 0$, $Q > 0$, which yields $F'(x_1) = 0$, and from (8) we obtain $\lambda_{1,2} = \pm j\sqrt{\epsilon^{-1} - b}$, $\lambda_3 = 0$. Thus, the Hopf bifurcation occurs at $a = 0$. See an example in Fig. 2, top panel, with

$$\omega = \text{Im}(\lambda_{1,2}) = \sqrt{\epsilon^{-1} - b} = 9.9997. \tag{9}$$

It is known that (8) has a pair of complex conjugate solutions if the following condition is satisfied: $\Delta \equiv -4P^3R + P^2Q^2 - 4Q^3 + 18PQR - 27R^2 < 0$. For the MMOs the third solution of (8) must be negative.

In the vicinity of the fold of the critical manifold we can approximate the system's dynamics by changing the coordinates

$$x_1 = \sqrt{\epsilon}\bar{x}_1, \qquad x_2 = \epsilon\bar{x}_2, \qquad x_3 = \sqrt{\epsilon}\bar{x}_3, \qquad t = \bar{t}\sqrt{\epsilon} \tag{10}$$

to obtain the following system from (2):

$$\begin{aligned} \bar{x}_1' &= -\bar{x}_2 + \alpha\bar{x}_1^2 + \beta\sqrt{\epsilon}\bar{x}_1^3, \\ \bar{x}_2' &= \bar{x}_1 - \bar{x}_3, \\ \bar{x}_3' &= \epsilon(\bar{a} - \bar{b}\epsilon\bar{x}_2). \end{aligned} \tag{11}$$

Since $\epsilon \ll 0$, ignoring the terms with ϵ in (11) yields

$$\begin{aligned} \bar{x}_1' &= -\bar{x}_2 + \alpha\bar{x}_1^2, \\ \bar{x}_2' &= \bar{x}_1 - \bar{x}_3^c \end{aligned} \tag{12}$$

with $\bar{x}_3^c = \text{const}$. By linearizing (12) we obtain oscillating $\bar{x}_1$ and $\bar{x}_2$ with frequency $\bar{\omega} = 1$ (in $\bar{t}$). Thus, the system (2) oscillates around the origin with $\omega = 1/\sqrt{\epsilon}$ (in t), which is very close to the estimate obtained from the $\lambda_{1,2}$ above.
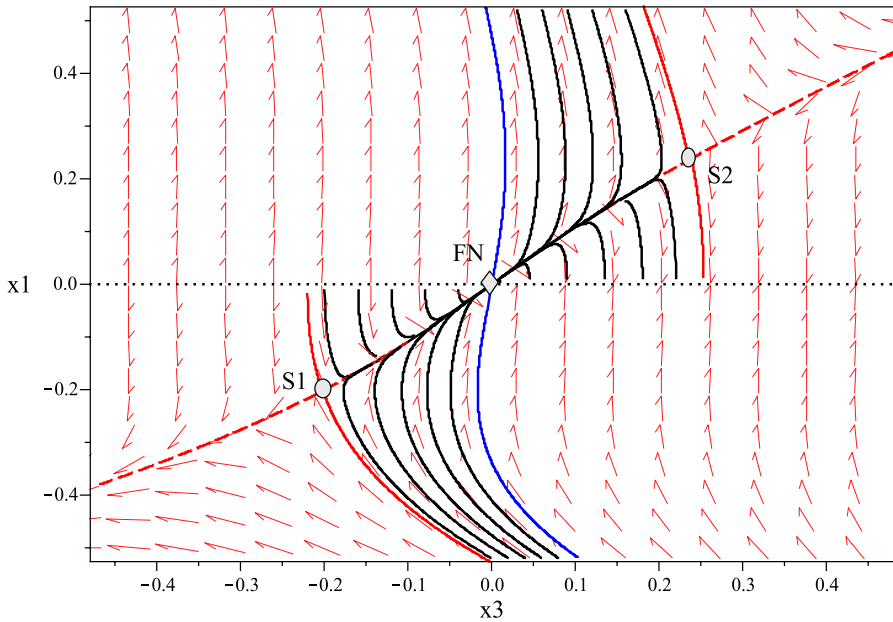
Fig. 8 (Color online) The flow of the *reduced* system (4) near a folded node *FN* for $a = 0.00035$ and $b = 0.005$. The x_1 axis is *the fold curve* and *the blue trajectory* is the *strong canard*. All *the black trajectories* are tangent to the *weak canard* at *FN*. The directions of the *blue* (angle 89.94°) and *black* (angle 45.03°) *trajectories* at *FN* are the eigendirections associated with λ_1 and λ_2, respectively. *S1* and *S2* are two saddles with coordinates $x_1 = x_3$ and $\beta x_1^3 + \alpha x_1^2 = a/b$. The sector bounded by the fold curve, the solid orbits of *S1* and *S2*, and the *blue* curve contains *singular canards* crossing *FN* from $x_1 < 0$ to $x_1 > 0$

The *desingularized* system (5) can be written as

$$x_1' = x_1 - x_3,$$
$$x_3' = \left(a - bF(x_1)\right)F'(x_1) \tag{13}$$
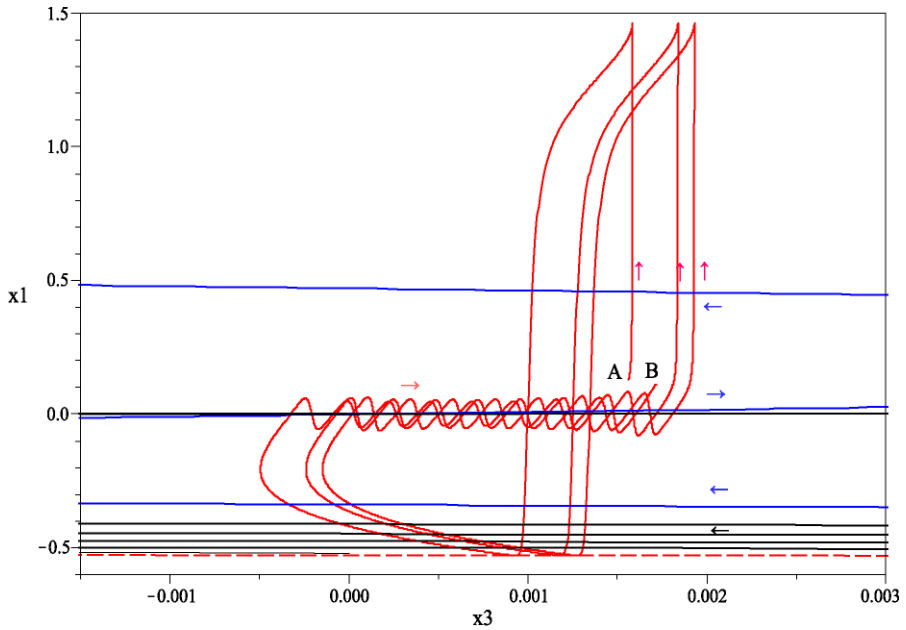
with the eigenvalues

$$\lambda_{1,2} = \left\{1 \pm \sqrt{1 - 4\left(\left(a - bF(x_1)\right)F'(x_1)\right)'}\right\}/2.$$

System (13) has two folded singularities at $(0, 0)$ and $(-2\alpha/(3\beta), -2\alpha/(3\beta))$ (obtained from $F'(x_1) = 0$ and $x_3 = x_1$). Further simplification of $\lambda_{1,2}$ at these folded singularities gives
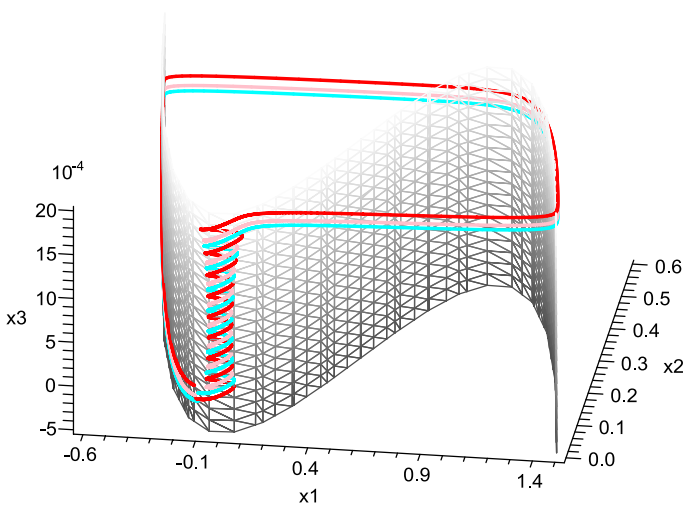
$$\lambda_{1,2} = \left\{1 \pm \sqrt{1 - 8a\alpha}\right\}/2 \quad \text{at } (0, 0)$$

and

$$\lambda_{1,2} = \frac{1}{2}\left\{1 \pm \sqrt{1 + 8a\alpha - \frac{32b\alpha^4}{27\beta^2}}\right\} \quad \text{at } \left(\frac{-2\alpha}{3\beta}, \frac{-2\alpha}{3\beta}\right).$$

Fig. 9 The flow of (2) for $a = 0.00035$, $b = 0.005$, $\epsilon = 0.01$, $\alpha = 1.5$, and $\beta = -1$ in the vicinity of the folded node *FN* in Fig. 8 with the trajectory twisted around the weak canard

Fig. 10 (Color online) MMOs $1^7(cyan)1^8(red)1^7(pink)$ for (2) with $a = 0.00035$, $b = 0.005$

The singularity $(-2\alpha/(3\beta), -2\alpha/(3\beta))$ is a folded node if $4b\alpha^3/(27\beta^2) - 1/(8\alpha) < a < 4b\alpha^3/(27\beta^2)$. The analysis in [9, 18] shows that for any fixed b system (2) is in the MMOs mode if $a < b\alpha^3/(18\beta^2)$. If we have $b\alpha^3/(18\beta^2) < 4b\alpha^3/(27\beta^2) - 1/(8\alpha)$, or equivalently $b > 27\beta^2/(20\alpha^4)$, then there are no MMOs since the max-
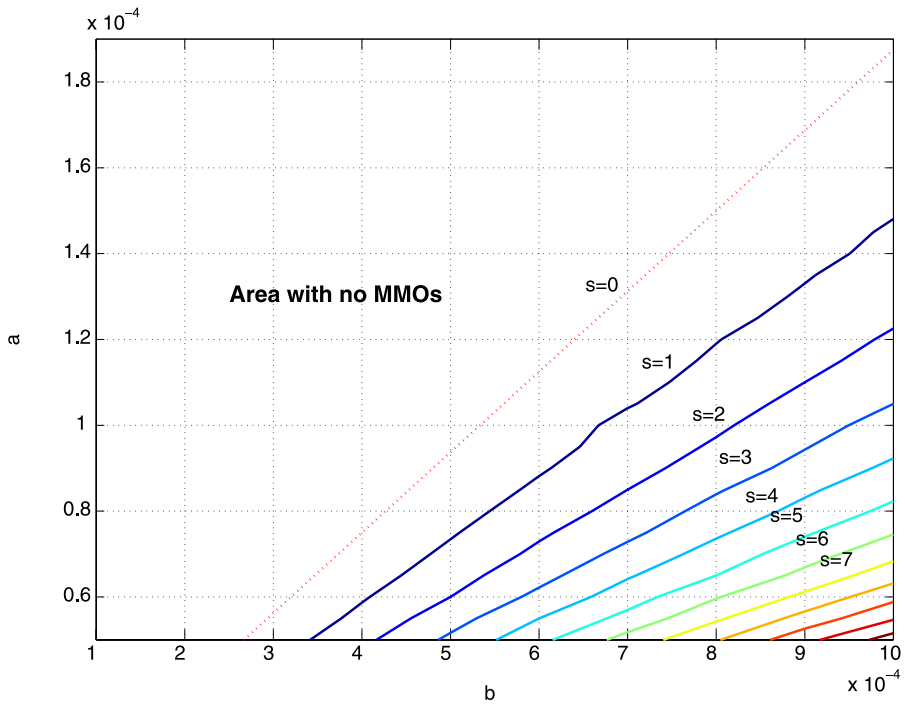
Fig. 11 Lines of constant average s values obtained by numerical simulation of (2) with 10 or more cycles 1^s

imum value of a for MMOs falls in the range where (2) has a folded focus rather than a folded node. For $a > b\alpha^3/(18\beta^2)$ MMOs cease to exist and (2) is in the pure relaxation mode (1^0 oscillations). Figure 7 shows how various types of responses of (2) depend on a.

The flow around the origin (point *FN*) of the reduced system is illustrated in Fig. 8. The MMOs twisted around the weak canard of (2) in the vicinity of the folded node *FN* in Fig. 8 are shown from various perspectives in Figs. 9 and 10. The sequence $1^71^81^7$ begins at point A and ends at B in Fig. 9.

Figure 11 shows the values of s obtained by numerical calculations. These s values are the *average* values obtained by considering at least 10 cycles of the form 1^s for each pair of discrete points (a, b). It is well known that for certain sets of parameters a and b, the dynamics of (2) can be of the form $1^{s_1}1^{s_2}1^{s_3}$ with s_1, s_2, s_3 being three consecutive integers, not necessarily in an increasing or decreasing order. For example, it is possible to have the sequence $1^31^11^2$. Such a sequence, for the purpose of creating Fig. 11, is considered to be equivalent to the stable *average* 1^2 sequence, i.e., one LAO with two SAOs. Also, the third graph in Fig. 2 with the dynamics 1^21^4 is considered to be of the *average* type 1^3 and the first graph in Fig. 4 with the sequence $2^2 = 1^01^2$ is of the *average* type 1^1.

The numerically obtained Fig. 11 confirms the analytical estimation in [9] of the lengths of the *sectors of rotation*, (or RS^j, $j = 0, 1, \ldots$), for the *secondary canard solutions*, i.e., solutions with small oscillations. These lengths are estimated to be con-

stant and independent of s, the number of small oscillations. The lengths are equivalent (for fixed values of a) to the distance between the straight lines of constant s values. However, for an increasing s (roughly speaking, for $s > 5$ in Fig. 11) one can see a uniform decrease of the distance between the lines of constant s for a fixed value of a. This is expected due to high-order corrections. Krupa et al. [9] estimate the constant length of RS^j in terms of the change of variable x_3 as $\Delta x_3 \sim 2a\epsilon^{3/2}\sqrt{-2\ln\epsilon}$.

Our numerical calculations also confirm the conjecture in [9] that L^s with either $L > 2$, $s \geq 2$ or $L \geq 2$, $s > 2$ is not possible for (2).

5 Conclusions

We have analyzed modified Chua's circuits with MMOs. The MMO mechanism is due to the presence of a nonlinear resistor with a cubic nonlinearity, linear controlled element, and a constant source. The linear controlled element and the constant source determine the *Farey sequence L^s* of MMOs. The existence of MMOs can be explained as a combination of the singular canard solutions at a fold point, canard explosion, relaxation oscillations, and a special return mechanism.

References

1. J. Abshagen, J.M. Lopez, F. Marques, G. Pfister, Bursting dynamics due to a homoclinic cascade in Taylor–Couette flow. J. Fluid Mech. **613**, 357–384 (2008)
2. M. Brøns, M. Krupa, M. Wechselberger, Mixed mode oscillations due to the generalized canard phenomenon. Fields Inst. Commun. **49**, 39–63 (2006)
3. D. Cafagna, G. Grassi, Generation of chaotic beats in a modified Chua's circuit, Part I: Dynamical behavior & Part II: Circuit design. Nonlinear Dyn. **44**, 91–108 (2005)
4. L.O. Chua, http://www.scholarpedia.org/article/Chua_circuit
5. Focus issue, Mixed mode oscillations: experiment, computation, and analysis. Chaos **18** (2008)
6. M.T.M. Koper, Bifurcation of mixed-mode oscillations in a three-variable autonomous Van der Pol-Duffing model with a cross-shaped phase diagram. Physica D **80**, 72–94 (1995)
7. M. Krupa, P. Szmolyan, Extending geometric singular perturbation theory to nonhyperbolic points—fold and canard points in two dimensions. SIAM J. Math. Anal. **33**, 286–314 (2001)
8. M. Krupa, P. Szmolyan, Relaxation oscillation and canard explosion. J. Differ. Equ. **174**, 312–368 (2001)
9. M. Krupa, N. Popovic, N. Kopell, Mixed-mode oscillations in three time-scale systems: a prototypical example. SIAM J. Appl. Dyn. Syst. **7**, 361–420 (2008)
10. R. Li, Z. Duan, B. Wang, G. Chen, A modified Chua's circuit with an attraction-repulsion function. Int. J. Bifurc. Chaos (IJBC) **18**, 1865–1888 (2008)
11. W. Marszalek, Fold points and singularities in Hall MHD differential-algebraic equations. IEEE Trans. Plasma Sci. **37**, 254–260 (2009)
12. W. Marszalek, Z.W. Trzaska, New solutions of resistive MHD systems with singularity induced bifurcations. IEEE Trans. Plasma Sci. **35**, 509–515 (2007)
13. W. Marszalek, T. Amdeberhan, R. Riaza, Singularity crossing phenomena in DAEs: a two-phase fluid flow application case study. Comput. Math. Appl. **49**, 303–319 (2005)
14. R. Riaza, S.L. Campbell, W. Marszalek, On singular equilibria of index-1 DAEs. Circuits Syst. Signal Process. **19**, 131–157 (2000)
15. P. Szmolyan, M. Wechselberger, Canards in $\mathbf{R}^3$. J. Differ. Equ. **177**, 419–453 (2001)

16. F. Tang, L. Wang, An adaptive active control for the modified Chua's circuit. Phys. Lett. A **346**, 342–346 (2005)
17. Q. Wang, Y. Chen, Generalized Q-S (lag, anticipated and complete) synchronization in modified Chua's circuit and Hindmarsh-Rose systems. Appl. Math. Comput. **181**, 48–56 (2006)
18. M. Wechselberger, Existence and bifurcations of canards in R^3 in the case of a folded node. SIAM J. Appl. Dyn. Syst. **4**, 101–139 (2005)